Optimization of electrolysis conditions for Ti film electrodeposition from water-soluble KF–KCl molten salts

Norikawa, Yutaro; Yasuda, Kouji; Nohira, Toshiyuki

Optimization of Electrolysis Conditions for Ti Film Electrodeposition from Water-Soluble KF–KCl Molten Salts

Yutaro Norikawa,[1] Kouji Yasuda,[2,3,*] and Toshiyuki Nohira[1,*,z]

[1]*Institute of Advanced Energy, Kyoto University, Gokasho, Uji, Kyoto 611-0011, Japan*
[2]*Agency for Health, Safety and Environment, Kyoto University, Yoshida-Hommachi, Sakyo-ku, Kyoto 606-8501, Japan*
[3]*Graduate School of Energy Science, Kyoto University, Yoshida-Hommachi, Sakyo-ku, Kyoto 606-8501, Japan*

Optimized conditions for Ti film electrodeposition were investigated in water-soluble KF–KCl (45:55 mol%) molten salt at 923 K. K_3TiF_6 was prepared in the melt via a comproportionation reaction between K_2TiF_6 and Ti sponges. The K_3TiF_6 solubility was determined to be 1.48 mol%. Galvanostatic electrolysis was conducted on Ni plate substrates at various K_3TiF_6 concentrations (0.28, 0.70, and 1.43 mol%) and current densities (25–150 mA cm^{-2}). Surface and cross-sectional scanning electron microscopy observations showed that adherent, compact, and smooth Ti films were obtained at higher K_3TiF_6 concentrations and lower current densities. A corrosion test was conducted for the Ti-coated Ni plate using linear sweep voltammetry, which showed that the Ti films have no cracks or voids.

 [DOI: 10.1149/2.1291914jes]

Manuscript submitted July 22, 2019; revised manuscript received September 17, 2019. Published October 15, 2019.

Titanium metal (Ti) has superior properties such as high corrosion and heat resistance and biocompatibility. Therefore, Ti metal is utilized in the manufacturing of aircraft, chemical plants, biological implants, etc. However, its high production cost and poor workability have prevented more widespread use. Thus, development of a new manufacturing process is an urgent demand.

Because many of Ti metal's superior properties are based on its surface characteristics, these can be provided by Ti metal plating on general substrates such as Ni, Fe and carbon. Because of the advantages of a higher deposition rate and shape flexibility compared to those of dry processes, Ti metal electrodeposition is a promising method and has been investigated using high-temperature molten salts.[1–17] In most cases, Ti films were obtained from fluoride-containing molten salts.[12–17] Ti films with a comparatively smooth surface were obtained in molten LiF–NaF–KF at 873–923 K by Robin et al.[12,13] and at 823–1023 K by Lepinay et al.[14] The necessity of a high fluoride-ion concentration for Ti film electrodeposition with a smooth surface was proved in Song et al.; the addition of KF salt to molten KCl–NaCl resulted in Ti metal with fine crystal grains.[9] However, a problem in the use of fluoride-based molten salts is removal of the adhered salts on the Ti film surface. This problem is caused by the low solubility of fluoride salts in water (LiF: 0.13 g, NaF: 4.13 g, MgF_2: 0.13 g, and CaF_2: 0.0016 g at 298 K per 100 g H_2O).[18]

Recently, we proposed a new process for Ti electrodeposition using a KF–KCl eutectic melt as an electrolyte.[19] The advantage using KF–KCl is its high solubility in water (102.0 g and 35.9 g for KF and KCl per 100 g H_2O, respectively)[18] enabling the removal of solidified salt by water washing. In addition, KF–KCl at the eutectic composition has a high fluoride-ion concentration (45 mol%) and its melting point is comparatively low (878 K).[20] We already investigated the electrochemical behavior of Ti(III) ions in KF–KCl molten salt at 923 K.[21] Ti(III) ions were synthesized in the melt by adding K_2TiF_6 and Ti sponge, wherein the following reaction proceeds.

$$6KF + Ti + 3K_2TiF_6 \rightarrow 4K_3TiF_6 \quad [1]$$

The oxidation of Ti(III) to Ti(IV) is a reversible electrochemical process with a standard formal redox potential of 1.82 V vs. K^+/K.[21] Ti(III) ion reduction to metallic Ti occurs at approximately 0.33 V.[21]

In the present study, the effects of Ti(III) ion concentration and current density on the Ti deposit morphology were investigated. First, the solubility of Ti(III) ions, i.e., K_3TiF_6, was determined using inductively coupled plasma-atomic emission spectrometry (ICP-AES). Second, the optimal conditions for electrodepositing adherent, compact, and smooth Ti films were evaluated via scanning electron microscopy (SEM) observations of the deposits prepared by galvanostatic electrolysis at various K_3TiF_6 concentrations and current densities. Finally, the corrosion resistance of the Ti-coated Ni plate was measured in artificial seawater via linear sweep voltammetry.

Experimental

Electrodeposition of Ti.—Reagent-grade KF (FUJIFILM Wako Pure Chemical Corp., >99.0%) and KCl (FUJIFILM Wako Pure Chemical Corp., >99.5%) were mixed to the eutectic composition (molar ratio of KF:KCl = 45:55, melting point = 878 K,[20] 400 g) and loaded in a Ni crucible (Chiyoda Industry Manufacturing Plant Co. Ltd., outer diameter: 96 mm, height: 102 mm). The mixture in the crucible was first dried under vacuum at 453 K for over 72 h. The crucible was placed at the bottom of a stainless-steel vessel in an air-tight Kanthal container and further dried under a vacuum at 773 K for 24 h. The electrochemical measurements were conducted in a dry Ar atmosphere at 923 K in a glove box. After blank measurements in the KF–KCl, 0.20–1.50 mol% of K_2TiF_6 (Morita Chemical Industry Co. Ltd., >97.5%) and 0.13–1.00 mol% of Ti sponges (FUJIFILM Wako Pure Chemical Corp., >99%) were added to the melt. Here, the added amount of Ti sponge corresponds to approximately twice the amount necessary to generate Ti(III) ions from the added K_2TiF_6 according to Eq. 1.

Electrochemical measurements and galvanostatic electrolysis were conducted using a three-electrode method with an electrochemical measurement system (Hokuto Denko Corp., HZ-7000). The working electrode was a Ni plate (Nilaco Corp., 10 mm × 10 mm in size, thickness: 0.1 mm, 99.95%), a Mo flag (Nilaco Corp., diameter: 3.0 mm, thickness: 0.1 mm, 99.95%), a Ni flag (Nilaco Corp., diameter: 3.0 mm, thickness: 0.1 mm, 99.98%), or a Pt flag (Nilaco Corp., diameter: 3.0 mm, thickness: 0.1 mm, 99.98%). The structure of the flag electrodes was reported in our previous paper.[22] A Ti rod (Nilaco Corp., diameter: 3.0 mm, 99.5%) was used as the counter and reference electrodes. The reference electrode potential was calibrated with reference to a dynamic K^+/K potential estimated using cyclic voltammetry on a Mo flag.[22] The melt temperature was measured using a type-K thermocouple. The electrolyzed samples on the Ni plates were soaked in distilled water at room temperature for 10 min to remove the salt adhered on the deposits. The surface and cross-section of the samples were observed by SEM (Keyence Corp., VE-8800). Prior to

*Electrochemical Society Active Member.
zE-mail: nohira.toshiyuki.8r@kyoto-u.ac.jp

Table I. K_3TiF_6 concentration determined using ICP-AES in molten salt after additions of K_2TiF_6 and Ti sponge at 923 K.

Added K_2TiF_6/mol%	Added Ti/mol%	K_3TiF_6 concentration/mol%	
		Analyzed	Theoretical
0.20	0.13	0.28	0.27
0.50	0.33	0.70	0.67
1.00	0.67	1.43	1.36
1.50	1.00	1.48	2.05

the observation of the cross section, the samples were cut at the center and embedded in acrylic resin. Then, the samples were polished by a cross-section polisher (CP; Hitachi, Ltd., IM4000) and coated with Au using an ion-sputtering apparatus (Hitachi, Ltd., E-1010). The samples were analyzed by energy dispersive X-ray spectroscopy (EDX; AMETEK Co., Ltd., EDAX Genesis APEX2) and X-ray diffraction (XRD; Rigaku Corp., Ultima IV, Cu-$K\alpha$ line). The Ti ion concentration in the molten salt was determined using ICP-AES (Hitachi, Ltd., SPECTRO BLUE). A small portion of molten salt was sampled and dissolved in 50 ml of HNO_3 aq (pH = 1, prepared from Tama Chemical Corp., AA-100 grade, 68 wt%).

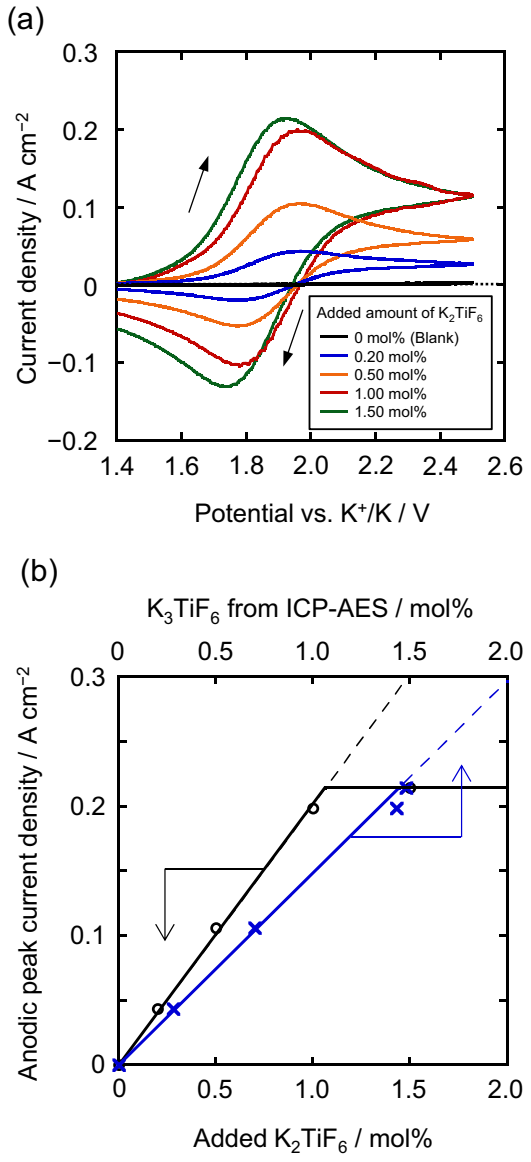

Figure 1. (a) Cyclic voltammograms at a Pt flag electrode in molten KF–KCl after adding various amounts of K_2TiF_6 (0, 0.20, 0.50, 1.00, and 1.50 mol%) and Ti sponge (0, 0.13, 0.33, 0.67, and 1.00 mol%) at 923 K. Scan rate: 0.50 V s^{-1}. (b) Dependence of anodic peak current density on the added amount of K_2TiF_6. The X-axis on the top denotes the K_3TiF_6 concentration determined using ICP-AES.

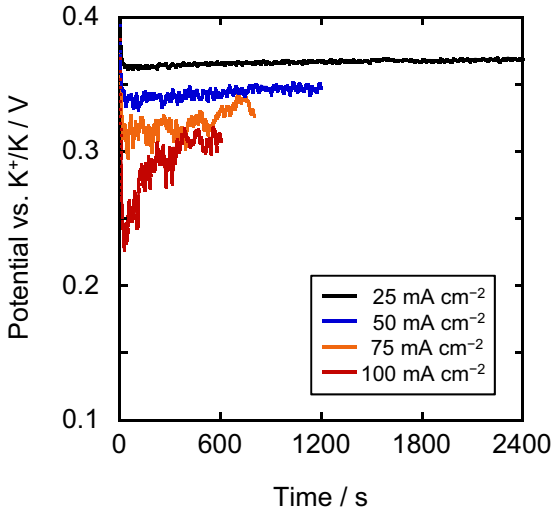

Figure 2. Potential transient curves during galvanostatic electrolysis at Ni electrodes at various current densities in molten KF–KCl–K_3TiF_6 (0.70 mol%) at 923 K.

Corrosion resistance test.—A total of 50 ml of artificial seawater (BizScience Co., Ltd., Aquamarine) was used as an electrolyte to measure the corrosion resistance of the Ti-coated Ni plate. In addition to this plate, Ni (Nilaco Corp., diameter: 3.0 mm, thickness: 0.1 mm, 99.98%) and Ti (Nilaco Corp., 10 mm × 10 mm, thickness: 0.1 mm, 99.5%) plates were also tested for comparison. As a reference electrode, an Ag/AgCl electrode in saturated KCl aq. was used. The potential was given with reference to the potential of the standard hydrogen electrode (SHE). A Pt plate (Nilaco Corp., 10 mm × 10 mm, thickness: 0.1 mm, 99.98%) was used as a counter electrode.

Results and Discussion

Ti(III) ion concentration.—Prior to electrodeposition, the Ti(III) ion concentration and electrochemical behavior were investigated. In our previous paper, we confirmed that nearly all of the Ti ions existed as Ti(III) ions in the KF–KCl eutectic melt after the addition of K_2TiF_6 and the Ti sponge.[21] Thus, the Ti concentration analyzed using ICP-AES was directly regarded as the Ti(III) concentration denoted as the K_3TiF_6 concentration formed according to Eq. 1.

Table I shows the K_3TiF_6 concentration at various added amounts of K_2TiF_6 and Ti sponge. The theoretical value of the K_3TiF_6 concentration was calculated according to Eq. 1 from the added amount of K_2TiF_6. Notably, the theoretical values in Table I are higher than the four-thirds of the added K_2TiF_6 because comproportionation reaction in Eq. 1 results in consumption of KF and decrease of the total moles of KF–KCl molten salt. When 0.20–1.00 mol% of K_2TiF_6 were added, the obtained K_3TiF_6 concentrations were nearly the same as the theoretical values. This agreement indicates nearly all of the added K_2TiF_6 was converted to K_3TiF_6 according to Eq. 1. However, with the addition of 1.50 mol% of K_2TiF_6, the obtained K_3TiF_6 concentration (1.48 mol%) was lower than the theoretical value (2.05 mol%). This result indicates that the solubility of K_3TiF_6 is 1.48 mol% in the KF–KCl eutectic melt at 923 K.

To further confirm the solubility, electrochemical measurement was conducted in KF–KCl after adding various amounts of K_2TiF_6 (0,

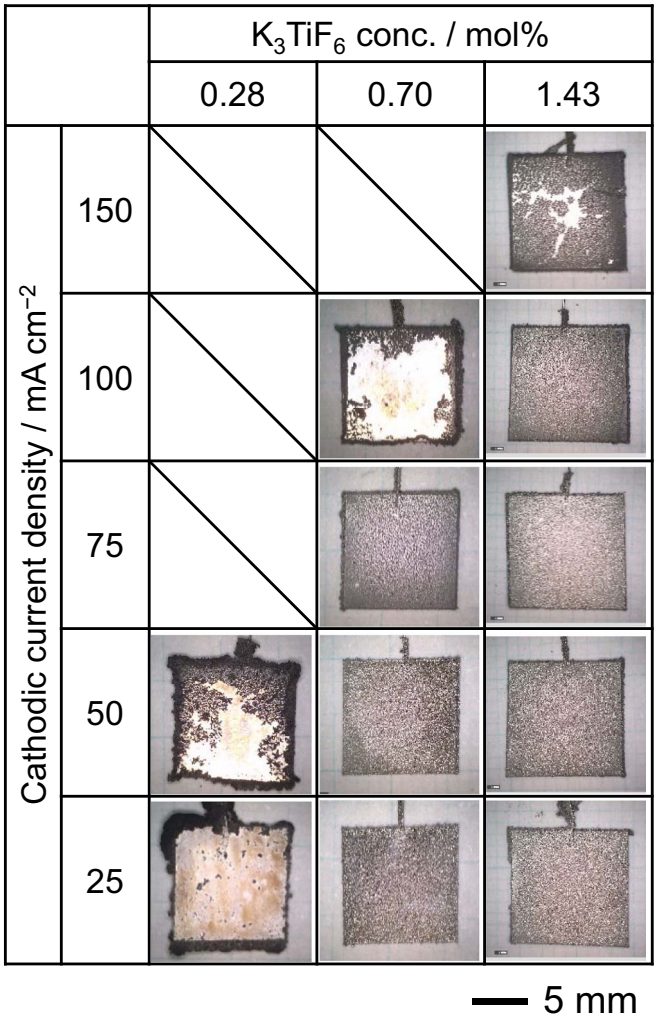

Figure 3. Optical images of the samples obtained by galvanostatic electrolysis at Ni plates in molten KF–KCl–K_3TiF_6 at 923 K. Charge density: 60 C cm^{-2}.

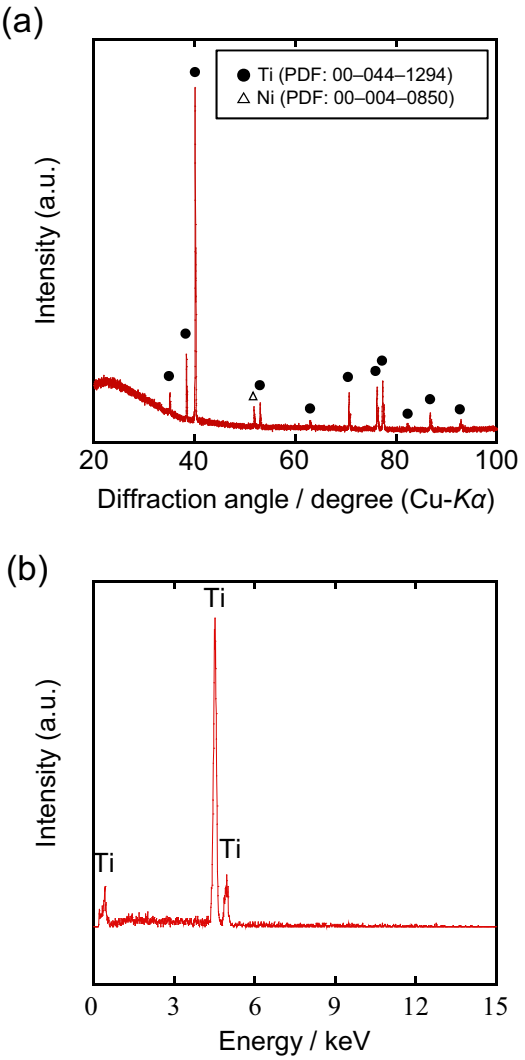

Figure 4. (a) XRD pattern and (b) EDX spectrum of the surface of the sample obtained by galvanostatic electrolysis at 25 mA cm^{-2} at a Ni plate in KF–KCl–K_3TiF_6 (0.70 mol%) at 923 K. Charge density: 60 C cm^{-2}.

0.20, 0.50, 1.00, and 1.50 mol%) and Ti sponge (0, 0.13, 0.33, 0.67, and 1.00 mol%). Fig. 1a shows cyclic voltammograms measured at a Pt flag electrode from 1.4 V in the positive direction. At each concentration, a pair of Ti(IV)/Ti(III) redox currents peaks is observed.[21] The anodic peak current density is plotted in Fig. 1b against the added amount of K_2TiF_6. The peak current linearly increases from blank to 1.0 mol% but negatively deviates from the linear relationship at 1.5 mol%. This behavior is explained by the Ti(III) ion solubility, i.e. the K_3TiF_6 solubility. The anodic peak current density is also plotted against the K_3TiF_6 concentration determined using ICP-AES in Fig. 1b. The current linearly increases with K_3TiF_6 concentration up to 1.48 mol%, which confirms that the K_3TiF_6 solubility is 1.48 mol%.

Morphology of electrodeposited Ti.—Galvanostatic electrolysis was conducted using an Ni plate electrode at various current densities from 25 to 150 mA cm^{-2} in KF–KCl–K_3TiF_6 (0.28, 0.70, and 1.43 mol%). Here, the reduction current was expressed as a positive value. The electric charge density was fixed at 60 C cm^{-2} for all electrolysis. The theoretical thickness of the electrodeposited Ti is 22 μm. Fig. 2 shows a comparison of the potential transient curves during electrolysis at 25–100 mA cm^{-2} in KF–KCl–K_3TiF_6 (0.70 mol%). The potential was more negative than 0.4 V vs. K^+/K from which the reduction current of Ti(III) to Ti metal was observed.[21] The potential is more negative at higher current density. Particularly, the potential becomes more negative than 0.25 V during the beginning at 100 mA cm^{-2}. At such a negative potential, K metal fog possibly occurs in the molten KF–KCl.[22] At 100 mA cm^{-2}, an increase in electrode area is also suggested because a positive shift in the potential was observed during the electrolysis.

Fig. 3 shows optical images of the obtained samples after washing with distilled water at room temperature for 10 min. At the highest current density for each K_3TiF_6 concentration, the obtained deposits were peeled from the Ni substrate during water washing because of poor adhesion. At low current densities of 0.70 and 1.43 mol% K_3TiF_6, silver-colored deposits were obtained. Fig. 4a shows the XRD pattern of the deposit obtained at 50 mA cm^{-2} at 0.70 mol% K_3TiF_6. No peaks other than metallic Ti and Ni substrate are observed, which suggests that the solidified salt was removed by water washing. To further confirm the salt removal, EDX analysis was conducted for the deposit as shown in Fig. 4b. Only Ti is detected and all the constituent elements of molten salt electrolyte (K, F, and Cl) are below the detection limits, which confirms complete removal of the solidified salts. At a lower concentration of 0.28 mol% K_3TiF_6, the appearance including the surface color is different from that of the other samples even at 25 mA cm^{-2}. Powder-like Ti was deposited at the edge parts, which is explained by the high local-current density at the edges. As the result, the Ti film on most parts of the substrate is as thin as a few micrometers, which was confirmed by cross-sectional SEM observation (data not shown).

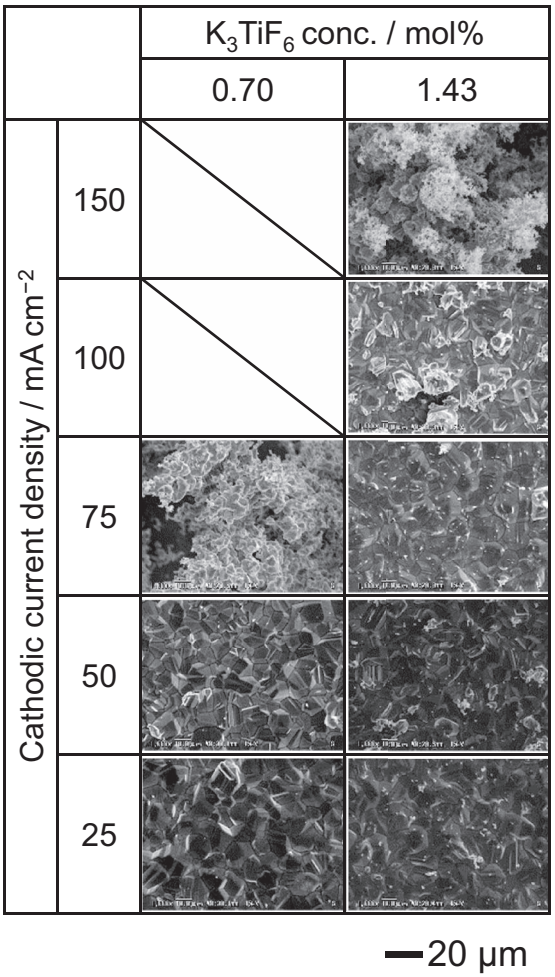

Figure 5. Surface SEM images of the samples obtained by galvanostatic electrolysis at Ni plates in KF–KCl–K_3TiF_6 at 923 K. Charge density: 60 C cm^{-2}.

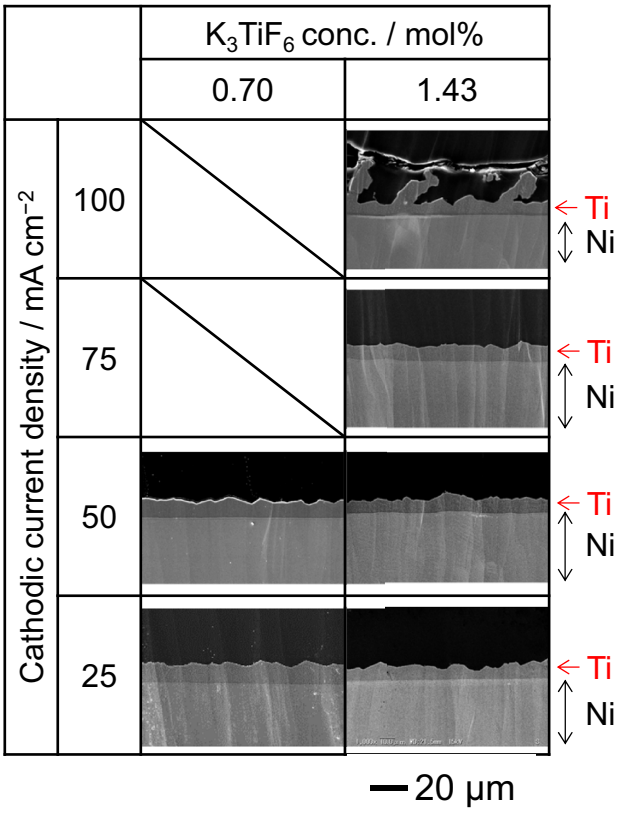

Figure 6. Cross-sectional SEM images of the samples obtained by galvanostatic electrolysis at Ni plates in KF–KCl–K_3TiF_6 at 923 K. Charge density: 60 C cm^{-2}.

Fig. 5 shows the surface SEM images and Fig. 6 shows the cross-sectional SEM images of the samples obtained in molten KF–KCl–K_3TiF_6 (0.70 and 1.43 mol%) at various current densities. Adherent, compact, and smooth Ti films are obtained at 25–50 mA cm^{-2} for 0.70 mol% K_3TiF_6 and at 25–75 mA cm^{-2} for 1.43 mol% K_3TiF_6. Under other conditions of higher current densities, coral-like or uneven Ti deposits are obtained. As a typical good Ti film, Fig. 7 shows the (a) surface and (b) cross-sectional SEM images of 50 mA cm^{-2} and 0.70 mol% K_3TiF_6. The thickness of the films on the center part of the substrate is 10–15 μm. Current efficiency calculated from the weight increase is as high as 90%. Despite the high current efficiency, the thickness of the Ti film at the center part is thinner than the theoretical value of 22 μm. This difference is possibly caused by current concentration on the electrode edges.

At higher current densities, for example, at 75 mA cm^{-2} for 0.70 mol% K_3TiF_6, coral-like growth perpendicular to the substrate is observed, as shown in Fig. 8a. In some cases, nodule Ti is found at the surface of the Ti films, as shown in Fig. 8b. The nodular and coral-like morphologies are because of the preferential deposition at convex parts of the Ti deposits.

In previous literature, Robin et al. reported that compact and well-crystallized Ti films were obtained from LiF–NaF–KF–K_3TiF_6 at 34.5–50 mA cm^{-2} at 873 and 973 K.[12] The conditions for obtaining good Ti films in LiF–NaF–KF–K_3TiF_6 are similar to those of the present study. Furthermore, the morphology of the obtained Ti films is nearly the same for both the LiF–NaF–KF and the KF–KCl systems.

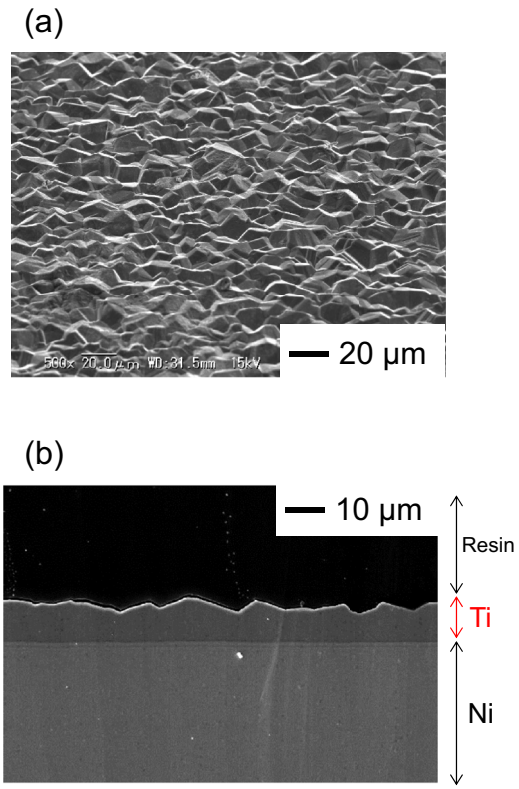

Figure 7. (a) Surface and (b) cross-sectional SEM images of the sample obtained by galvanostatic electrolysis at 50 mA cm^{-2} at a Ni plate in KF–KCl–K_3TiF_6 (0.70 mol%) at 923 K. Charge density: 60 C cm^{-2}.

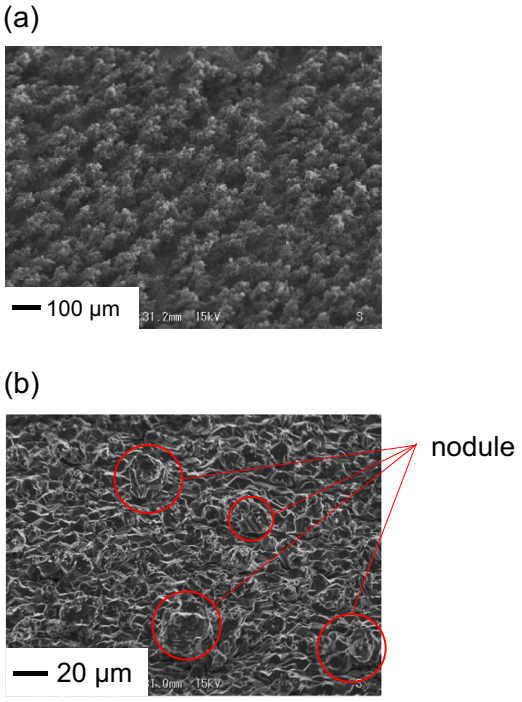

Figure 8. Surface SEM images of the samples obtained by galvanostatic electrolysis at Ni plates at (a) 75 mA cm^{-2} in KF–KCl–K_3TiF_6 (0.70 mol%) and (b) 100 mA cm^{-2} in KF–KCl–K_3TiF_6 (1.43 mol%) at 923 K. Charge density: 60 C cm^{-2}.

Thus, Ti films having a similar quality as the molten LiF–NaF–KF system can be obtained from the water-soluble KF–KCl molten salt.

Corrosion resistance test.—To evaluate the corrosion resistance of the Ti-coated Ni plate, linear sweep voltammetry was conducted in artificial seawater at 295 K. The Ti-coated Ni plate was prepared by galvanostatic electrolysis at 25 mA cm^{-2} for 40 min in KF–KCl–K_3TiF_6 (1.43 mol%). The estimated thicknesses of the Ti films are 10–15 μm. Fig. 9 shows the obtained voltammograms in which the potential was swept from the open-circuit potential to 2.0 V vs. SHE at a scan rate of 1 mV s^{-1}. For comparison, the voltammograms at the Ni and Ti plates are also shown. At the Ni plate electrode, the anodic current resulting from Ni dissolution rapidly increases from the open-circuit potential. However, for the Ti-coated sample, the anodic current reaches a limit of 0.1 mA cm^{-2} until 2.0 V. This behavior is similar to that of the Ti plate. Such excellent corrosion resistance is a result of the formation of passivation oxide films.[23,24] The results demonstrate that the electrodeposited Ti films completely coated the Ni substrate without any voids. The different open-circuit potential and the obtained currents between the Ti plate and Ti-coated sample possibly relate to the amount of impure elements.

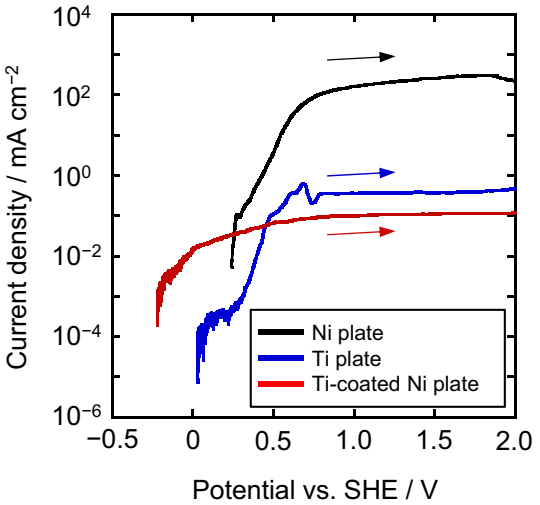

Figure 9. A linear sweep voltammogram of Ti-coated Ni in artificial seawater at 295 K. Scan rate: 1 mV s^{-1}. The Ti-coated Ni plate was prepared by galvanostatic electrolysis at 25 mA cm^{-2} for 40 min in molten KF–KCl–K_3TiF_6 (1.43 mol%). Linear sweep voltammograms of the Ni and Ti plates are shown for comparison.

Conclusions

The optimal condition for the electrodeposition of adherent, compact, and smooth Ti films in KF–KCl–K_3TiF_6 at 923 K was investigated. The solubility of K_3TiF_6 was confirmed to be 1.48 mol% using ICP-AES. Galvanostatic electrolysis was conducted on Ni plate substrates at various K_3TiF_6 concentrations (0.28, 0.70, and 1.43 mol%) and current densities (25–150 mA cm^{-2}). Surface and cross-sectional SEM observations showed that adherent, compact, and smooth Ti films were obtained at 25–50 mA cm^{-2} for 0.70 mol% K_3TiF_6 and at 25–75 mA cm^{-2} for 1.43 mol% K_3TiF_6. Finally, linear sweep voltammetry at a Ti-coated Ni plate electrode showed high corrosion resistance in artificial seawater at 295 K, proving that no cracks or voids exist in the Ti films.

Acknowledgments

Parts of this study were conducted as collaborative research with Sumitomo Electric Industries, Ltd.

ORCID

Kouji Yasuda https://orcid.org/0000-0001-5656-5359
Toshiyuki Nohira https://orcid.org/0000-0002-4053-554X

References

1. M. B. Alpert, F. J. Schultz, and W. F. Sullivan, *J. Electrochem. Soc.*, **104**, 555 (1957).
2. B. J. Fortin, J. G. Wurm, L. Gravel, and R. J. A. Potvin, *J. Electrochem. Soc.*, **106**, 423 (1959).
3. J. A. Menzies, D. L. Hill, G. J. Hills, L. Young, and J. O'M. Bockris, *J. Electroanal. Chem.*, **1**, 161 (1959).
4. S. Tokumoto, E. Tanaka, and K. Ogisu, *J. Metals*, **27**, 18 (1975).
5. G. M. Haarberg, W. Rolland, A. Sterten, and J. Thonstad, *J. Appl. Electrochem.*, **23**, 217 (1993).
6. H. Takamura, I. Ohno, and H. Numata, *J. Jpn. Inst. Metals*, **60**, 388 (1996).
7. J. G. Gussone and J. M. Hausmann, *J. Appl. Electrochem.*, **41**, 657 (2011).
8. X. Ning, H. Asheim, H. Ren, S. Jiao, and H. Zhu, *Metall. Mater. Trans. B*, **42**, 1181 (2011).
9. Y. Song, S. Jiao, L. Hu, and Z. Guo, *Metall. Mater. Trans. B*, **47**, 804 (2016).
10. T. Uda, T. H. Okabe, Y. Waseda, and Y. Awakura, *Sci. Technol. Adv. Mater.*, **7**, 490 (2006).
11. M. H. Kang, J. Song, H. Zhu, and S. Jiao, *Metall. Mater. Trans. B*, **46**, 162 (2015).
12. A. Robin, J. D. Lepinay, and M. J. Barbier, *J. Electroanal. Chem.*, **230**, 125 (1987).
13. A. Robin and R. B. Ribeiro, *J. Appl. Electrochem.*, **30**, 239 (2000).
14. J. D. Lepinay, J. Bouteillon, S. Traore, D. Renaud, and M. J. Barbier, *J. Appl. Electrochem.*, **17**, 294 (1987).
15. D. Wei, M. Okido, and T. Oki, *J. Appl. Electrochem.*, **24**, 923 (1994).
16. J. H. Barner, P. Noye, A. Barhoun, and F. Lantelme, *J. Electrochem. Soc.*, **152**, C20 (2005).
17. V. V. Malyshev and D. B. Shakhnin, *Mater. Sci.*, **50**, 80 (2014).
18. J. R. Rumble, (Ed.), *CRC Handbook of Chemistry and Physics*, 99th ed., CRC Press, Boca Raton (2018).
19. Y. Norikawa, K. Yasuda, and T. Nohira, *Mater. Trans.*, **58**, 390 (2017).
20. L. P. Cook and H. F. McMurdie, Editors, *Phase Diagrams for Ceramists vol. VII*, The American Ceramic Society Inc., p. 509 (1989).
21. Y. Norikawa, K. Yasuda, and T. Nohira, *Electrochemistry*, **86**, 99 (2018).
22. K. Maeda, K. Yasuda, T. Nohira, R. Hagiwara, and T. Homma, *J. Electrochem. Soc.*, **162**, D444 (2015).
23. I. Dugdale and J. B. Cotton, *Corrosion Sci.*, **4**, 397 (1964).
24. F. A. Pose and E. G. Bohlmann, *Desalination*, **3**, 269 (1967).